

## Supplementary Information

### **MIL-101 supported CeO<sub>x</sub>-modified NiPt nanoparticles as a highly efficient catalyst toward complete dehydrogenation of hydrazine borane**

*Yaxuan Bai,<sup>a,b</sup> Yubo Liu,<sup>a,b</sup> Henan Shang,<sup>a,b</sup> SiJia Li<sup>a,b\*</sup> and Jinsheng Liang<sup>a,b</sup>*

<sup>a</sup>Key Laboratory of Special Functional Materials for Ecological Environment and Information (Hebei University of Technology), Ministry of Education, Tianjin 300130, China

<sup>b</sup>Institute of Power Source and Ecomaterials Science, Hebei University of Technology, Tianjin 300130, China

E-mail: [lisj@hebut.edu.cn](mailto:lisj@hebut.edu.cn)

## Part 1 Supplementary experimental details

### *Materials*

All chemicals are commercially available and can be used without further purification. Hydrazine hemisulfate salt ( $\text{N}_2\text{H}_4 \cdot 1/2\text{H}_2\text{SO}_4$ , Sigma Aldrich Chemistry Co., Ltd.,  $\geq 98\%$ ), sodium borohydride ( $\text{NaBH}_4$ , Sinopharm Chemical Reagent Co., Ltd., 96%), 1,4-dioxane ( $\text{C}_4\text{H}_8\text{O}_2$ , Shanghai Maklin Biochemical Co., Ltd.,  $\geq 99\%$ ), n-pentane ( $\text{C}_5\text{H}_{12}$ , Shanghai Maklin Biochemical Co., Ltd.,  $\geq 99\%$ ), chromic nitrate nonahydrate ( $\text{Cr}(\text{NO}_3)_3 \cdot 9\text{H}_2\text{O}$ , Shanghai Aladdin Biochemical Technology Co., Ltd., 99%), terephthalic acid ( $\text{HO}_2\text{CC}_6\text{H}_4\text{CO}_2\text{H}$ , Shanghai Aladdin Biochemical Technology Co., Ltd., 99%), aqueous hydrofluoric acid (HF, Shanghai Aladdin Biochemical Technology Co., Ltd.,  $\geq 40\%$ ), ammonium fluoride ( $\text{NH}_4\text{F}$ , Shanghai Aladdin Biochemical Technology Co., Ltd., 98%), nickel (II) chloride hexahydrate ( $\text{NiCl}_2 \cdot 6\text{H}_2\text{O}$ , Shanghai Aladdin Biochemical Technology Co., Ltd.,  $>98\%$ ), potassium (II) tetrachloroplatinate ( $\text{K}_2\text{PtCl}_4$ , Shanghai Aladdin Biochemical Technology Co., Ltd.,  $\geq 99.9\%$ , Pt  $\geq 46\%$ ), cerium (III) nitrate hexahydrate ( $\text{Ce}(\text{NO}_3)_3 \cdot 6\text{H}_2\text{O}$ , Shanghai Aladdin Biochemical Technology Co., Ltd., 99.5%), zinc nitrate hexahydrate ( $\text{Zn}(\text{NO}_3)_2 \cdot 6\text{H}_2\text{O}$ , Alfa Aesar, 99%), cobalt nitrate hexahydrate ( $\text{Co}(\text{NO}_3)_2 \cdot 6\text{H}_2\text{O}$ , Shanghai Aladdin Biochemical Technology Co., Ltd.,  $>99\%$ ), zirconium tetrachloride ( $\text{ZrCl}_4$ , Shanghai Aladdin Biochemical Technology Co., Ltd., 98%), 2-methylimidazole ( $\text{C}_4\text{H}_6\text{N}_2$ , Shanghai Aladdin Biochemical Technology Co., Ltd., 98%), sodium hydroxide (NaOH, Shanghai Aladdin Biochemical Technology Co., Ltd., 97%), N,N-Dimethylformamide (DMF,  $\text{C}_3\text{H}_7\text{NO}$ , Shanghai Aladdin Biochemical Technology Co., Ltd.,  $>99.9\%$ ), methanol ( $\text{CH}_3\text{OH}$ , Shanghai Maklin Biochemical Co., Ltd., 99.5%), ethanol ( $\text{C}_2\text{H}_5\text{OH}$ , Tianjin Huihang Chemical Technology Co., Ltd.,  $\geq 99.7\%$ ). Deionized water with the specific resistance of  $18.25 \text{ M}\Omega \cdot \text{cm}$  is obtained by reversed osmosis followed by ion-exchange and filtration.

### ***Synthesis of ZIF-8***

ZIF-8 was synthesized according to the reported procedure.<sup>S1</sup>  $\text{Zn}(\text{NO}_3)_2 \cdot 6\text{H}_2\text{O}$  (1.5 g) was dissolved in 70 mL methanol to form the solution A. The 2-methylimidazole (3.3 g) was dissolved in 70 mL methanol to form the solution B. Solution B was added dropwise to the solution A, and stirred at room temperature for 24 h. The product was centrifuged, washed with methanol 3 times and dried under vacuum at 323 K overnight.

### ***Synthesis of ZIF-67***

ZIF-67 was synthesized according to the reported procedure.<sup>S2</sup>  $\text{Co}(\text{NO}_3)_2 \cdot 6\text{H}_2\text{O}$  (1.18 g) was dissolved in 60 mL methanol to form the solution A. The 2-methylimidazole (2.0 g) was dissolved in 20 mL methanol to form the solution B. Solution B was added dropwise to the solution A, and stirred at room temperature for 24 h. The product was centrifuged, washed with methanol 3 times and dried under vacuum at 323 K overnight.

### ***Synthesis of UIO-66***

UIO-66 was synthesized according to the reported procedure.<sup>S3</sup>  $\text{ZrCl}_4$  (0.58 g) and terephthalic acid (0.415 g) were dispersed in 75 mL DMF. The above mixture was transferred to a 100 mL Teflon-liner autoclave and heated at 393 K for 24 h. After cooling to room temperature, the product was collected by centrifugation, washed with DMF 3 times and dried under vacuum at 323 K overnight.

### ***Synthesis of $\text{CeO}_2$ nanorods***

$\text{CeO}_2$  nanorods was synthesized according to the reported procedure.<sup>37</sup>  $\text{Ce}(\text{NO}_3)_3 \cdot 6\text{H}_2\text{O}$  (0.67 g) was dissolved in NaOH solution (9 M, 30 mL) under vigorous stirring. The suspension was transferred to a 50 mL Teflon-liner autoclave and heated at 413 K for 48 h. After the autoclave was cooled to room temperature, the  $\text{CeO}_2$  nanorods was collected by centrifugation, washed with  $\text{H}_2\text{O}$  and dried in air at 353 K overnight. The sample was labeled as  $\text{CeO}_2$  (rod).

### ***Synthesis of CeO<sub>2</sub> nanocubes***

CeO<sub>2</sub> nanocubes was synthesized according to the reported procedure.<sup>52</sup> Ce(NO<sub>3</sub>)<sub>3</sub>·6H<sub>2</sub>O (1.72 g) was dissolved in 20 mL H<sub>2</sub>O, then add NaOH solution (10 M, 60 mL) into the above solution. The obtained solution was stirred for 30 min at room temperature and transferred into 100 mL Teflon-lined autoclave and heated at 403 K for 48 h. Followed by cooling to room temperature and transferred into a beaker, ultrasonic for 1 h. The CeO<sub>2</sub> nanocubes was collected by centrifugation, washed with H<sub>2</sub>O several times and dried at 373 K overnight. The sample was labeled as CeO<sub>2</sub> (cube).

### ***Synthesis of catalysts***

Ni<sub>0.9</sub>Pt<sub>0.1</sub>-CeO<sub>x</sub>/MIL-101 (14 mol% Ce) was synthesized by a simple impregnated reduction at room temperature. In a typical experiment, MIL-101 (40 mg) was first dispersed in 4 mL H<sub>2</sub>O by stirring and sonication. Then impregnate the NiCl<sub>2</sub>·6H<sub>2</sub>O (0.1 M, 0.9 mL), K<sub>2</sub>PtCl<sub>4</sub> (0.1 M, 0.1 mL) and Ce(NO<sub>3</sub>)<sub>3</sub>·6H<sub>2</sub>O (0.0163 M, 1 mL) aqueous solution into the MIL-101 dispersion with magnetic stirring for 10 min. Subsequently, 1 mL of an aqueous solution containing 30 mg of NaBH<sub>4</sub> was added to the above dispersion, stirred and reduced to no bubbles, and the black product was obtained as Ni<sub>0.9</sub>Pt<sub>0.1</sub>-CeO<sub>x</sub>/MIL-101 (14 mol% Ce) catalyst.

The Ni<sub>0.9</sub>Pt<sub>0.1</sub>-CeO<sub>x</sub>/ZIF-8, Ni<sub>0.9</sub>Pt<sub>0.1</sub>-CeO<sub>x</sub>/ZIF-67, and Ni<sub>0.9</sub>Pt<sub>0.1</sub>-CeO<sub>x</sub>/UiO-66 catalysts with different MOFs supports were also synthesized according to the procedure similar to the above, the only difference was to replace MIL-101 with ZIF-8, ZIF-67 and UiO-66 respectively.

The Ni<sub>0.9</sub>Pt<sub>0.1</sub>-CeO<sub>x</sub> (rod)/MIL-101 and Ni<sub>0.9</sub>Pt<sub>0.1</sub>-CeO<sub>x</sub> (cube)/MIL-101 catalysts modified by CeO<sub>2</sub> with different morphologies were also synthesized as the mentioned method, in which the dose of CeO<sub>2</sub> (rod) and CeO<sub>2</sub> (cube) were both 0.0028 g.

For comparison, Ni<sub>0.9</sub>Pt<sub>0.1</sub>/MIL-101 and unsupported Ni<sub>0.9</sub>Pt<sub>0.1</sub>-CeO<sub>x</sub> catalysts were synthesized according to the procedure similar to the above. The difference was that there was

no  $\text{Ce}(\text{NO}_3)_3 \cdot 6\text{H}_2\text{O}$  precursor solution for the former and the latter without the introduction of MIL-101. In addition, for the  $\text{Ni}_{0.9}\text{Pt}_{0.1}$  NPs sample without support,  $\text{NiCl}_2 \cdot 6\text{H}_2\text{O}$  (0.1 M, 0.9 mL) and  $\text{K}_2\text{PtCl}_4$  (0.1 M, 0.1 mL) were dispersed in 5 mL  $\text{H}_2\text{O}$ , 1 mL of an aqueous solution containing 30 mg of  $\text{NaBH}_4$  was added with stirring until no bubbles were generated. Similarly, for the MIL-101 without metal loading and  $\text{CeO}_x$  samples, the MIL-101 (40 mg) and  $\text{Ce}(\text{NO}_3)_3 \cdot 6\text{H}_2\text{O}$  (0.1 M, 1 mL) were dispersed in 6 mL and 5 mL  $\text{H}_2\text{O}$ , respectively. Subsequently, 1 mL of an aqueous solution containing 30 mg of  $\text{NaBH}_4$  was added and stirred until no bubbles were generated to obtain MIL-101 and  $\text{CeO}_x$  samples.

$\text{Ni}_y\text{Pt}_{1-y}\text{-CeO}_x/\text{MIL-101}$  ( $y = 0, 0.1, 0.3, 0.5, 0.7, 0.9, 1$ ) catalysts with different Ni/Pt molar ratios were synthesized by changing the molar content of  $\text{NiCl}_2 \cdot 6\text{H}_2\text{O}$  and  $\text{K}_2\text{PtCl}_4$  according to the same process described above.

In addition,  $\text{Ni}_{0.9}\text{Pt}_{0.1}\text{-CeO}_x/\text{MIL-101}$  catalysts with different amounts of  $\text{CeO}_x$  and support were prepared by changing the addition amount of  $\text{Ce}(\text{NO}_3)_3 \cdot 6\text{H}_2\text{O}$  (4 mol%, 9 mol%, 14 mol%, 19 mol%, 24 mol%) and MIL-101 (10 mg, 20 mg, 30 mg, 40 mg, 50 mg, 60 mg), respectively in the same way as above.

### ***Catalytic activities***

The reaction device used to measure the  $\text{H}_2$  production from HB dehydrogenation is as follows. Typically, the aqueous suspension of the as-prepared  $\text{Ni}_{0.9}\text{Pt}_{0.1}\text{-CeO}_x/\text{MIL-101}$  catalyst (0.1 mmol of metal catalyst, 7 mL) was dissolved in a two-necked round bottom flask (50 mL) placed in the water bath at 323 K under ambient atmosphere. One neck of the flask was connected to a typical water-filled graduated gas burette and the other was connected to a pressure-equalization funnel to introduce  $\text{NaOH}$  (10 M, 1 mL) and HB (0.5 M, 2 mL) in sequence. The catalytic reaction was started when the HB aqueous solution was added into the catalyst suspension in the flask with magnetic stirring. The evolution of gas was monitored using the gas burette and recorded at consequent times.

For the other comparative catalysts synthesized, the catalytic activities for HB dehydrogenation were also applied as the above method, the molar ratio of metal/HB ( $n_{Ni+Pt}/n_{HB}$ ) of all metal-containing catalysts during the reaction was constant at 0.1. Only the temperature of the corresponding water bath needs to be adjusted for testing the influence of temperature and evaluate the activation energy of HB dehydrogenation.

### ***Recycle stability test***

For the recycle stability test, after the previous run of catalytic dehydrogenation of HB was completed, another equivalent of HB (0.5 M, 2 mL) and the corresponding quantity of NaOH were subsequently added to the flask. The released gas was also monitored by the gas burette. The recycle stability test for the synthesized catalyst was carried out at 323 K.

### ***Calculation methods:***

Based on the number of moles of metal, calculate the total turnover frequency (TOF) value of HB according to the following equation:

$$TOF = \frac{n_{H_2}}{n_{metal}t} \quad \text{Eq. (S1)}$$

Where  $n_{metal}$  is the mole number of active metal atoms (Ni+Pt) in the catalyst,  $n_{H_2}$  is the mole number of the generated H<sub>2</sub>,  $t$  is the total time to complete the reaction.

The relationship of the temperature and the reaction rate (full conversion) was followed Arrhenius behavior. The Arrhenius' reaction rate equation can be written as follows:

$$\ln TOF = \ln A - E_a/RT \quad \text{Eq. (S2)}$$

Where A is the reaction constant.

## Part 2 Supplementary Figures and Tables

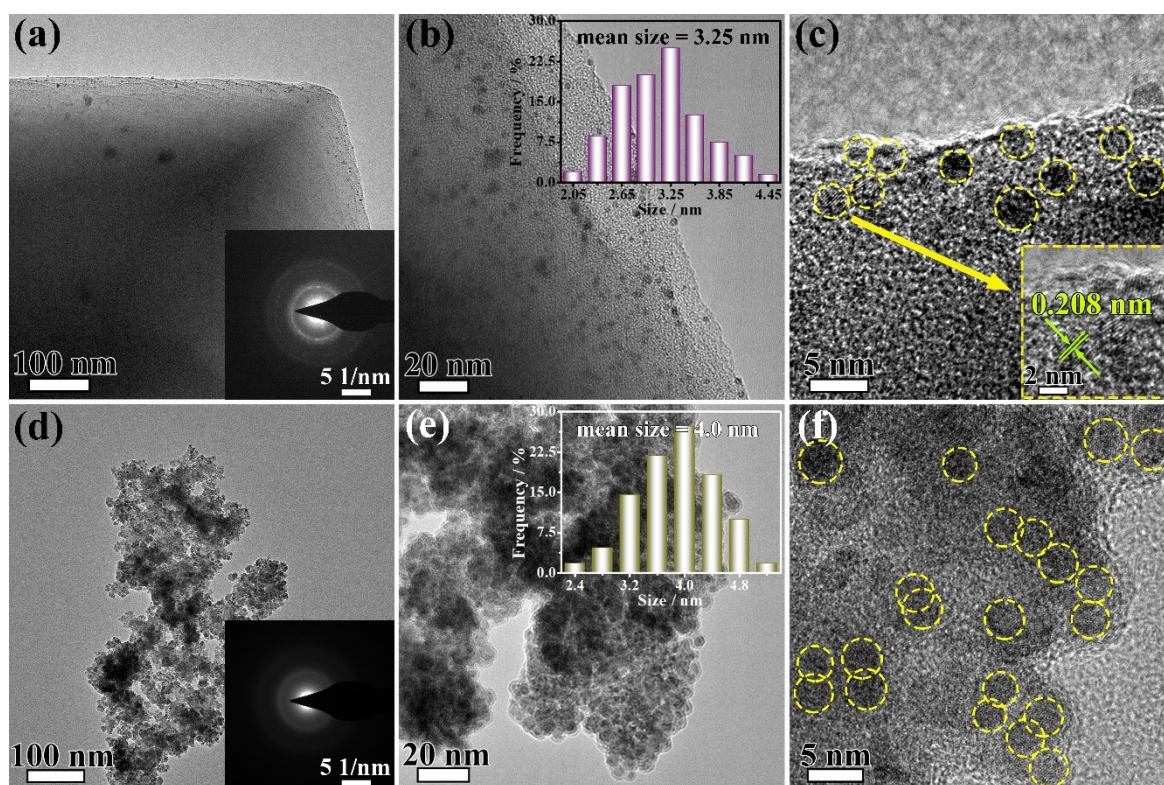


**Figure S1.** (a) Low-resolution (inset is the corresponding SAED pattern), (b) medium-resolution (inset is the corresponding size distribution) and (c) high-resolution TEM images of  $\text{Ni}_{0.9}\text{Pt}_{0.1}/\text{MIL-101}$ ; (d) low-resolution (inset is the corresponding SAED pattern), (e) medium-resolution (inset is the corresponding size distribution) and (f) high-resolution TEM images of  $\text{Ni}_{0.9}\text{Pt}_{0.1}-\text{CeO}_x$ .

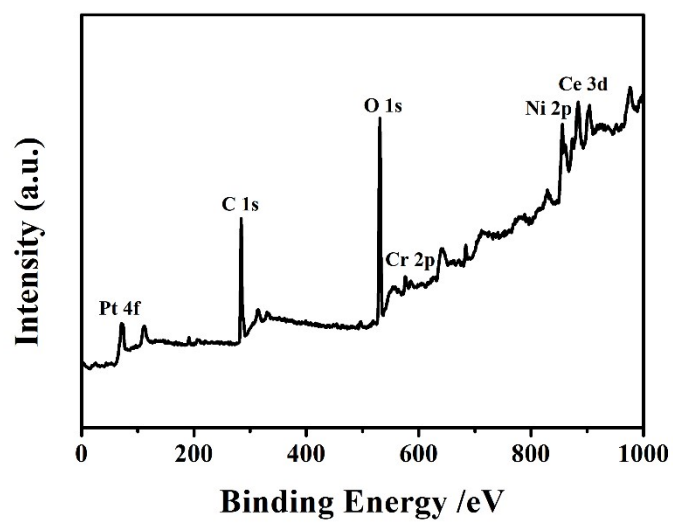


**Figure S2.** The full XPS spectrum for Ni<sub>0.9</sub>Pt<sub>0.1</sub>-CeO<sub>x</sub>/MIL-101.



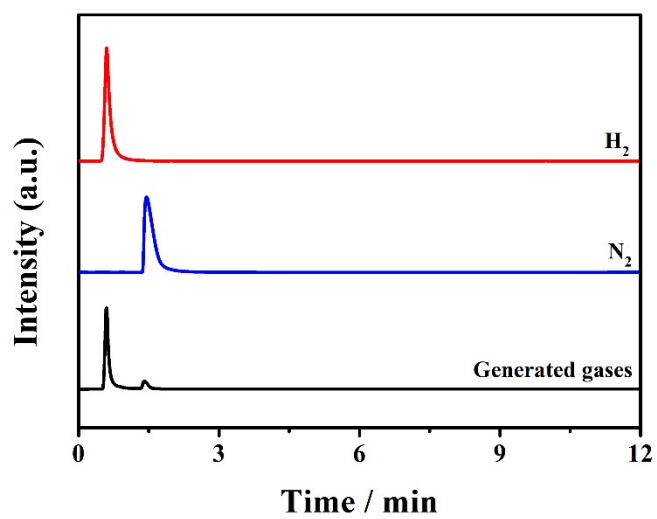


**Figure S3.** GC spectrum using TCD for the evolved gas from HB aqueous solution (0.5 M, 2.0 mL) over Ni<sub>0.9</sub>Pt<sub>0.1</sub>-CeO<sub>x</sub>/MIL-101 at 323 K (black trace), the commercial pure N<sub>2</sub> (blue trace) and H<sub>2</sub> (red trace).

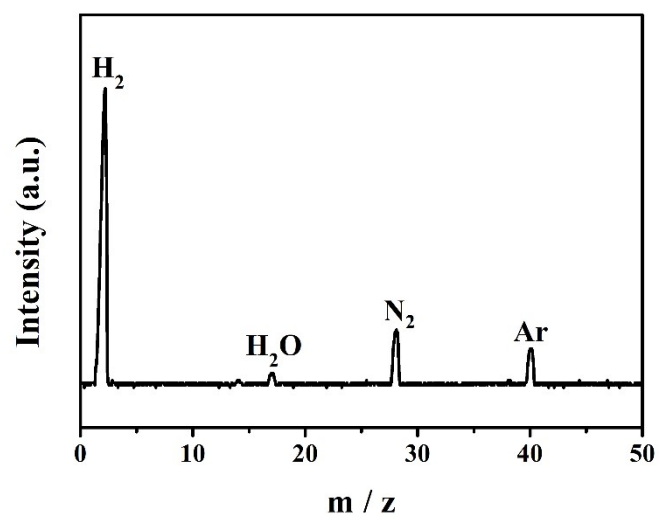


**Figure S4.** MS of released gases from the complete decomposition of HB catalyzed by Ni<sub>0.9</sub>Pt<sub>0.1</sub>-CeO<sub>x</sub>/MIL-101 catalyst in Ar atmosphere at 323 K.

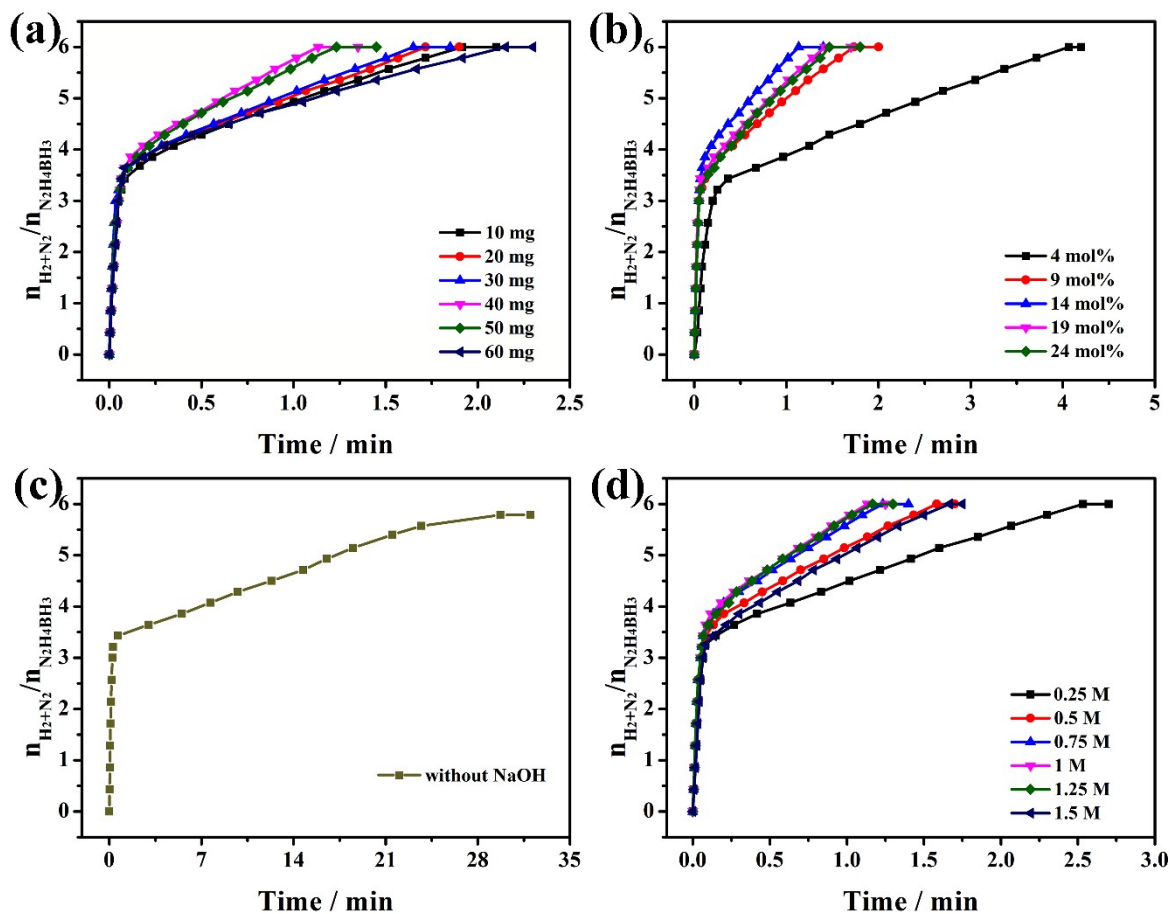


**Figure S5.** Gas generation from the decomposition of HB (0.5 M, 2.0 mL) versus time over  $\text{Ni}_{0.9}\text{Pt}_{0.1}\text{-CeO}_x/\text{MIL-101}$  (a) with different dosage of MIL-101, (b) with different molar content of  $\text{CeO}_x$ , (c) without NaOH and (d) with different concentration of NaOH at 323 K. ( $n_{\text{Ni+Pt}}/n_{\text{HB}} = 0.0897$ ).

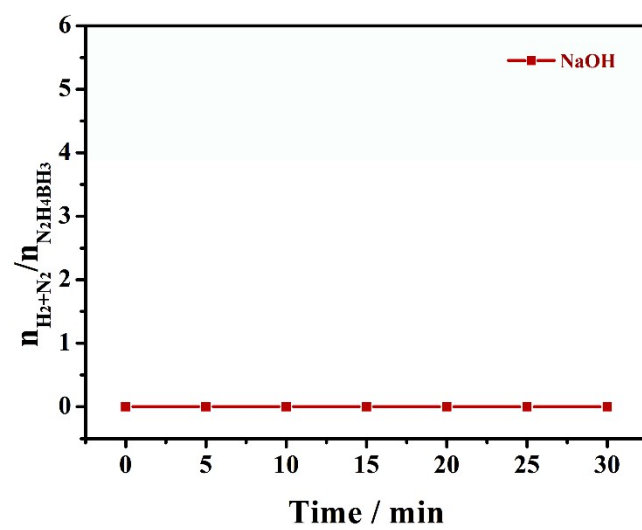


**Figure S6.** Gas generation from the decomposition of HB (0.5 M, 2.0 mL) versus time over NaOH at 323 K.

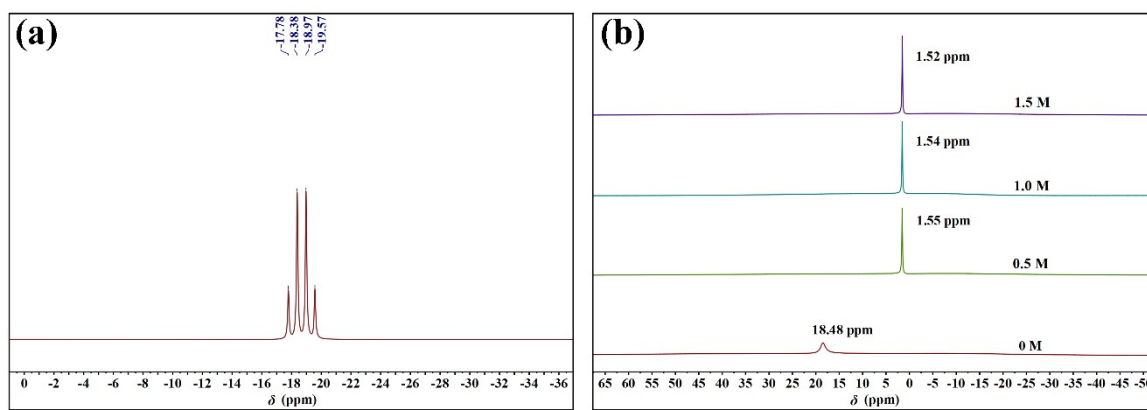


**Figure S7.** Solution-state  $^{11}\text{B}$  NMR spectra of (a) the synthesized HB in  $\text{CD}_3\text{CN}$  and (b) the solution after the catalytic reaction with different concentrations of NaOH in  $\text{D}_2\text{O}$ .

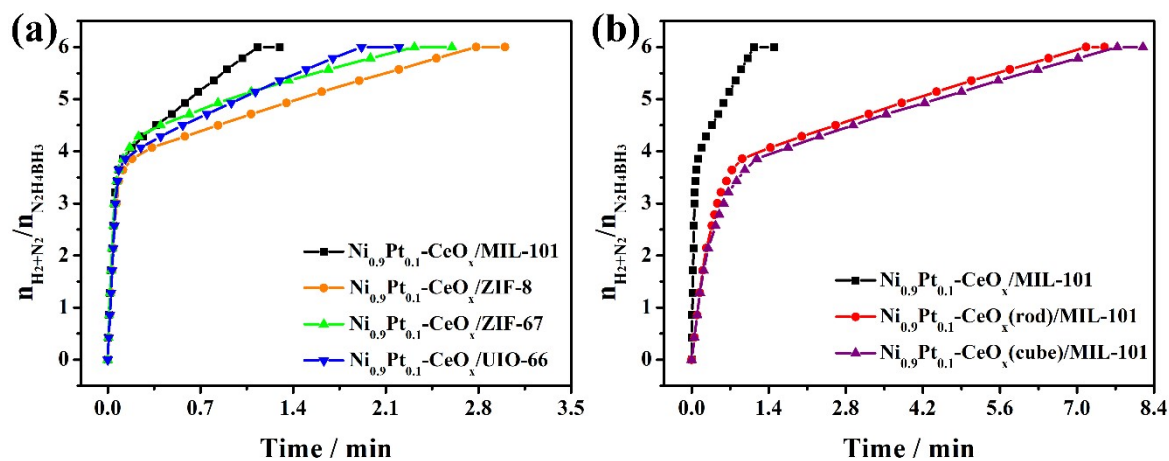


**Figure S8.** (a) Gas generation from the decomposition of HB (0.5 M, 2.0 mL) versus time over  $\text{Ni}_{0.9}\text{Pt}_{0.1}\text{-CeO}_x/\text{MIL-101}$ ,  $\text{Ni}_{0.9}\text{Pt}_{0.1}\text{-CeO}_x/\text{ZIF-8}$ ,  $\text{Ni}_{0.9}\text{Pt}_{0.1}\text{-CeO}_x/\text{ZIF-67}$  and  $\text{Ni}_{0.9}\text{Pt}_{0.1}\text{-CeO}_x/\text{UIO-66}$ ; (b) gas generation from the decomposition of HB (0.5 M, 2.0 mL) versus time over  $\text{Ni}_{0.9}\text{Pt}_{0.1}\text{-CeO}_x/\text{MIL-101}$ ,  $\text{Ni}_{0.9}\text{Pt}_{0.1}\text{-CeO}_x$  (rod)/MIL-101 and  $\text{Ni}_{0.9}\text{Pt}_{0.1}\text{-CeO}_x$  (cube)/MIL-101.

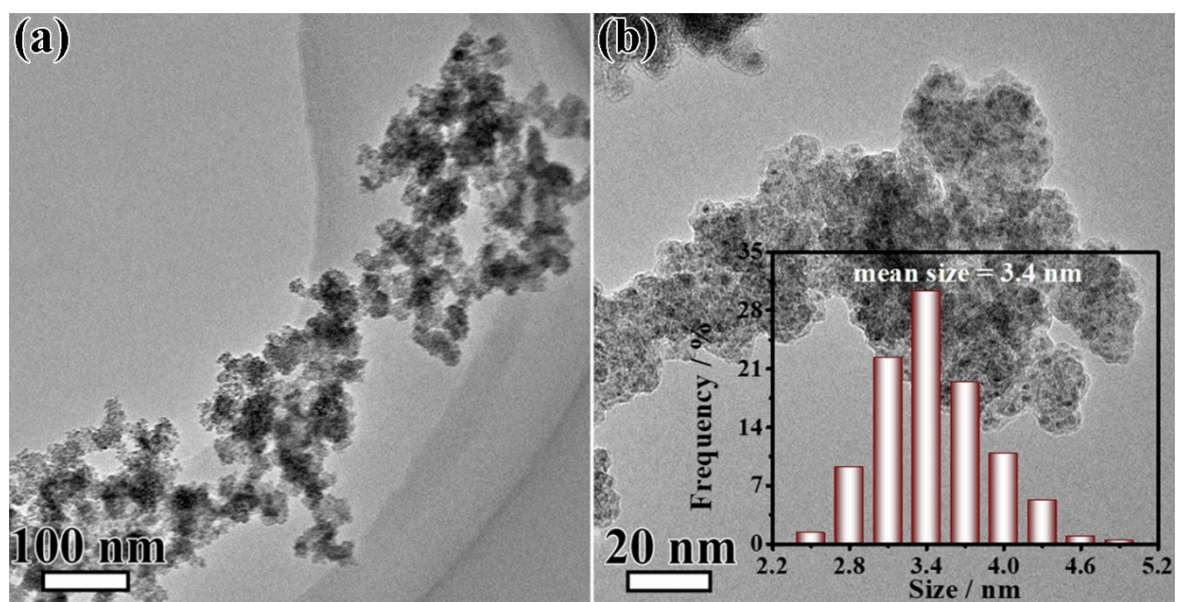


**Figure S9.** (a) Low-resolution and (b) medium-resolution TEM images (inset is the corresponding size distribution) of  $\text{Ni}_{0.9}\text{Pt}_{0.1}\text{-CeO}_x/\text{MIL-101}$  after the reaction.

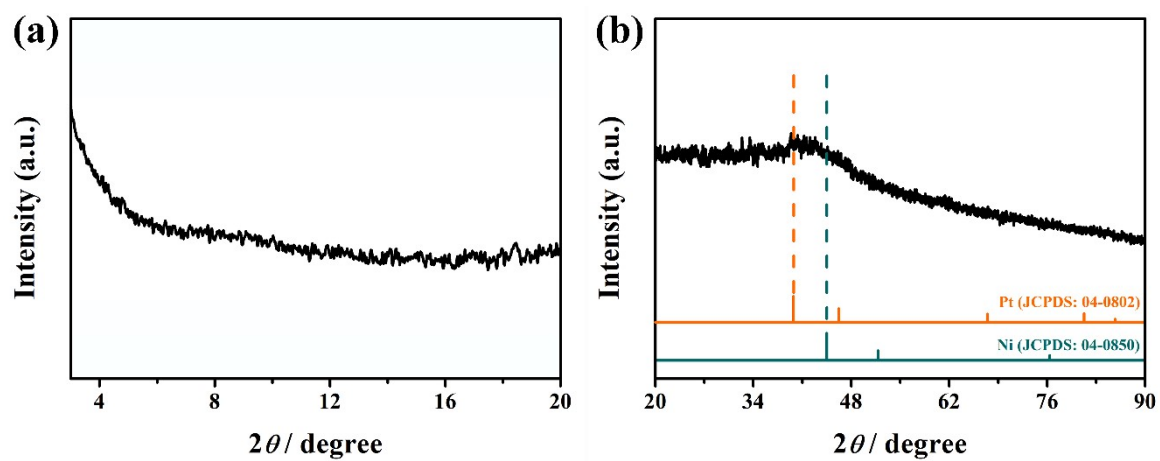


**Figure S10.** (a) Low-angle and (b) wide-angle XRD patterns of  $\text{Ni}_{0.9}\text{Pt}_{0.1}\text{-CeO}_x/\text{MIL-101}$  after reaction.



**Table S1.** BET specific surface areas, total pore volumes and average pore diameter of the as-synthesized MIL-101 support and Ni<sub>0.9</sub>Pt<sub>0.1</sub>-CeO<sub>x</sub>/MIL-101 catalyst.

| <b>Sample</b>  | <b>BET surface area<br/>(m<sup>2</sup>·g<sup>-1</sup>)</b> | <b>Total pore volume<br/>(cm<sup>3</sup>·g<sup>-1</sup>)</b> | <b>Average pore<br/>diameter (nm)</b> |
|--|--|--|---------------------------------------|
| MIL-101  | 1063.49  | 0.79   | 2.36                                  |
| Ni <sub>0.9</sub> Pt <sub>0.1</sub> -CeO <sub>x</sub> /MIL-101 | 869.33   | 0.51   | 2.98                                  |

**Table S2.** Comparison of catalytic activity of different catalysts for HB dehydrogenation (references cited here refer those given in the main manuscript).

| Catalyst  | Temp. (K) | Reaction time (min) | $n(\text{H}_2+\text{N}_2)/n(\text{HB})$ | TOF ( $\text{h}^{-1}$ ) | Ref.      |
|---|-----------|---------------------|---|-------------------------|-----------|
| $\text{Ni}_{0.9}\text{Pt}_{0.1}\text{-CeO}_x/\text{MIL-101}$        | 323       | 1.13                | 6.0                                     | 2951.1                  | This work |
| $\text{Ni}_{0.22}@\text{Ir}_{0.78}/\text{OMS-2}$                    | 323       | None                | 6.0                                     | 2590                    | 38        |
| $\text{Ni}_{0.58}\text{Pt}_{0.42}/\text{graphene}$                  | 323       | 0.8                 | 6.0                                     | 2303                    | 12        |
| $\text{Rh}_{0.5}(\text{MoO}_x)_{0.5}$                               | 323       | 1.5                 | 6.0                                     | 2000                    | 39        |
| $\text{Ni}_{0.9}\text{Pt}_{0.1}/\text{MIL-101}/\text{rGO}$          | 323       | 1.9                 | 6.0                                     | 1578.9                  | 26        |
| $\text{Ni}_{0.9}\text{Pt}_{0.1}/\text{MIL-101\_A}$                  | 323       | 1.95                | 6.0                                     | 1515                    | 6         |
| $\text{Ni}_{0.75}\text{Ir}_{0.25}/\text{La}_2\text{O}_2\text{CO}_3$ | 323       | 2.4                 | 6.0                                     | 1250                    | 40        |
| $\text{Rh}_{0.8}\text{Ni}_{0.2}/\text{MIL-101}$                     | 323       | 2.5                 | 6.0                                     | 1200                    | 41        |
| $\text{Ni}_{0.9}\text{Pt}_{0.1}\text{-Cr}_2\text{O}_3$              | 323       | 2.5                 | 6.0                                     | 1200                    | 42        |
| $\text{Rh}_{0.8}\text{Ni}_{0.2}@\text{CeO}_x/\text{rGO}$            | 323       | 4.5                 | 6.0                                     | 666.7                   | 17        |
| $\text{Ni-MoO}_x/\text{BN}$   | 323       | 5                   | 6.0                                     | 600                     | 8         |
| $\text{Rh}_4\text{Ni}$  | 323       | 30                  | 6.0                                     | 90.9                    | 43        |
| $\text{Ni}_{0.36}\text{Fe}_{0.24}\text{Pd}_{0.4}/\text{MIL-101}$    | 323       | 25                  | 6.0                                     | 60                      | 10        |
| $\text{Ni}_{0.6}\text{Pd}_{0.4}\text{-MoO}_x$                       | 323       | 7.33                | 5.92                                    | 405                     | 44        |
| $\text{Ni}_{0.89}\text{Pt}_{0.11}$                                  | 323       | None                | 5.79                                    | 18                      | 16        |
| $\text{Ni}@\text{(RhNi-alloy)}/\text{Al}_2\text{O}_3$               | 323       | 40                  | 5.74                                    | 71.7                    | 18        |
| $\text{Ni}_5@\text{Pt}$   | 323       | 110                 | 4.5                                     | 2.3                     | 45        |
| $\text{Ni}_{0.7}\text{Pd}_{0.3}/\text{CTAB}$                        | 323       | 180                 | 4.3                                     | None                    | 46        |
| $\text{RhCl}_3$   | 323       | 180                 | 4.1                                     | 93.3                    | 9         |

**Table S3.** Catalysts composition determined by inductively coupled plasma optical emission spectroscopy (ICP-OES).

| <b>Catalyst</b>  | <b>Ni(mmol)</b> | <b>Pt(mmol)</b> | <b>Ce(mmol)</b> | <b>Ni:Pt<br/>(molar ratio)</b> |
|--|-----------------|-----------------|-----------------|--------------------------------|
| Ni-CeO <sub>x</sub> /MIL-101   | 0.0805          | 0               | 0.0136          | -                              |
| Ni <sub>0.9</sub> Pt <sub>0.1</sub> -CeO <sub>x</sub> /MIL-101                     | 0.0808          | 0.0089          | 0.0147          | 0.90:0.10                      |
| Ni <sub>0.7</sub> Pt <sub>0.3</sub> -CeO <sub>x</sub> /MIL-101                     | 0.0588          | 0.0265          | 0.0144          | 0.69:0.31                      |
| Ni <sub>0.5</sub> Pt <sub>0.5</sub> -CeO <sub>x</sub> /MIL-101                     | 0.0419          | 0.0418          | 0.0139          | 0.50:0.50                      |
| Ni <sub>0.3</sub> Pt <sub>0.7</sub> -CeO <sub>x</sub> /MIL-101                     | 0.0269          | 0.0566          | 0.0138          | 0.32:0.68                      |
| Ni <sub>0.1</sub> Pt <sub>0.9</sub> -CeO <sub>x</sub> /MIL-101                     | 0.0100          | 0.0735          | 0.0139          | 0.12:0.88                      |
| Pt-CeO <sub>x</sub> /MIL-101   | 0               | 0.0723          | 0.0121          | -                              |
| Ni <sub>0.9</sub> Pt <sub>0.1</sub> -CeO <sub>x</sub> /MIL-101<br>(after reaction) | 0.0454          | 0.0054          | 0.0090          | 0.89:0.11                      |

**Table S4.** Comparison of  $E_a$  values of different catalysts for HB dehydrogenation (references cited here refer those given in the main manuscript).

| Catalyst  | NaOH/M | $E_{a1}$ (kJ·mol <sup>-1</sup> ) | $E_{a2}$ (kJ·mol <sup>-1</sup> ) | Ref.      |
|---|--------|----------------------------------|----------------------------------|-----------|
| Ni <sub>0.9</sub> Pt <sub>0.1</sub> -CeO <sub>x</sub> /MIL-101                        | 1.0    | 10.5                             | 43.9                             | This work |
| Ni <sub>0.6</sub> Pd <sub>0.4</sub> -MoO <sub>x</sub>                                 | 0.75   | 49.7                             | 72.6                             | 44        |
| Ni <sub>0.22</sub> @Ir <sub>0.78</sub> /OSM-2   | 5.0    | 40.9                             | 63.4                             | 38        |
| Ni <sub>0.9</sub> Pt <sub>0.1</sub> -MoO <sub>x</sub> /NH <sub>2</sub> -N-rGO         | 1.5    | 36.1                             | 46.2                             | 48        |
| Ni <sub>60</sub> Pt <sub>40</sub> /MNC-800  | 1.0    | 32.2                             | 50.9                             | 7         |
| Ni <sub>0.36</sub> Fe <sub>0.24</sub> Pd <sub>0.4</sub> /MIL-101                      | 2.0    | 30.3                             | 58.1                             | 10        |
| Ni <sub>0.88</sub> Fe <sub>0.12</sub> /La(OH) <sub>3</sub>                            | 1.5    | 27.5                             | 58.2                             | 53        |
| Cu <sub>0.4</sub> Ni <sub>0.6</sub> Mo  | 2.0    | 19.8                             | 54.7                             | 54        |
| Ni <sub>0.9</sub> Pt <sub>0.1</sub> /MIL-101_A  | 0.5    | 18.6                             | 44.6                             | 6         |
| Rh <sub>0.5</sub> (MoO <sub>x</sub> ) <sub>0.5</sub>                                  | 2.0    | 18.6                             | 56.9                             | 39        |
| Ni <sub>0.9</sub> Pt <sub>0.1</sub> /MIL-101/rGO                                      | 1.0    | 17.6                             | 56.4                             | 26        |
| Rh <sub>0.8</sub> Ni <sub>0.2</sub> /MIL-101  | 0.5    | 17.5                             | 47.1                             | 41        |
| Rh <sub>0.8</sub> Ni <sub>0.2</sub> @CeO <sub>x</sub> /rGO                            | 0.5    | 17.4                             | 55.2                             | 17        |
| Raney Ni  | 1.0    | 17.1                             | 39.5                             | 55        |
| Ni <sub>0.75</sub> Ir <sub>0.25</sub> /La <sub>2</sub> O <sub>2</sub> CO <sub>3</sub> | 1.2    | 16.3                             | 57.7                             | 40        |

## References

- S1 S. X. Wu, W. H. Wang, Y. Z. Fang, X. J. Kong and J. H. Liu, *React. Kinet. Catal. Lett.*, 2017, **122**, 357-367.
- S2 J. N. Qin, S. B. Wang and X. C. Wang, *Appl. Catal., B*, 2017, **209**, 476-482.
- S3 F.-Z. Song, Q.-L. Zhu, X. C. Yang, W.-W. Zhan, P. Pachfule, N. Tsumori and Q. Xu, *Adv. Energy Mater.*, 2018, **8**, 1701416.